INFLUENCE OF NON-NEWTONIAN FLUID RHEOLOGY ON PIPE AND ANNULAR FLOW DYNAMICS IN RESERVOIR DEVELOPMENT

Muhammad Obeidat
•
Azerbaijan State Oil and Industry University
muhob1207@gmail.com

Abstract

During reservoir development, efficient fluid transport is very important for the optimization of production and minimization of operational costs. This study investigates the influence of non-Newtonian fluid properties on the flow behavior in pipes and in annuli. Unlike Newtonian fluids, the non-Newtonian fluids have much more complex rheological characteristics which include yield stress and power-law index, and those properties affect the overall fluid dynamics during production from the well and further fluid transport in the pipelines. Lack of consideration of non-Newtonian parameters during engineering calculations leads to different technical, economic and ecological risks. A full mathematical derivation of velocity distribution in pipes and in annuli for non-Newtonian fluids was presented. Based on the velocity distributions the formulas for flow rates have also been derived and the flow conditions for yield stress fluids have been shown. It has been demonstrated that yield stress fluids form a certain region in the middle of the flow that flows with maximum velocity but individual fluid layers within this region do not move relative to each other, so the velocity gradient is zero here. This region is referred to as core of the flow. The analysis has shown that in pipes the decrease of yield stress strongly increases velocity and decreases the radius of the core. The decrease of the consistency index significantly increases velocity. One of the most interesting observations is that the relationship between velocity and the power-law index depends on the pressure gradient. At low pressure gradients the increase of the power-law index increases the velocity, but at high pressure gradients the increase of the power-law index decreases the velocity. For annular flow the effect of those parameters is the same, however, the velocity for annular flow is much more sensitive to the pressure gradient and the yield stress.

Keywords: non-Newtonian fluids, Herschel-Bulkley model, Bingham model, fluid flow in pipes, fluid flow in annulus

I. Introduction

Non-Newtonian fluids are widely used in the oil and gas industry. Most of the oil reserves in the world today can be characterized as unconventional reserves a significant portion of which is made up of non-Newtonian fluids [1], [2]. The relevance of studying the behavior of non-Newtonian oils is growing nowadays as many experts believe that in the future most of the demand for oil will be fulfilled by non-Newtonian reserves [3]. Non-Newtonian fluids are also very common in drilling, as most of the drilling muds have non-Newtonian behavior [4].

The simplest definition of non-Newtonian fluids is that any fluid the flow of which cannot be described by the Newtonian law [5] is considered non-Newtonian. There is a certain set of parameters that are unique to non-Newtonian fluids which are:

- Yield stress. Fluids that have yield stress do not flow until the shear stress that occurs in them exceeds a certain value which is known as the yield stress [6].
- Power-law index. For some fluids the relationship between shear stress and velocity gradient is not linear and this nonlinearity is taken into account by a parameter known as the power-law index [7]
- Consistency index. For non-Newtonian fluids that have a power-law index that is not equal to 1, dynamic viscosity is replaced with the consistency index, the dimension of which is dependent on the power-law index [8].

A complete analysis of fluid flow is not possible without taking into account the boundary conditions. Some examples of practically encountered boundary conditions are upward flow of oil through the production tubing, horizontal flow of oil through long pipelines used for transport of hydrocarbons to large distances, downward flow of drilling mud through the drill pipe, upward flow of drilling mud through the annulus between the borehole wall and the drill pipe and etc.

Lack of consideration of non-Newtonian parameters during engineering calculations related to pipeline systems design means ignoring the influence of those parameters on the flow [9]. Obviously, this introduces several risks. Such risks might be technical (actual flow rate too far from the predicted one, the velocity profile in pipe is different from the predicted profile, etc.), economical (the necessary volume of fluids is not delivered through the transport pipeline) and ecological (failure of fluid transport facilities leading to ecological harm). The best mitigation of those risks is consideration of as many flow parameters as possible (the ones that have impact on the flow) during engineering calculations.

Several authors have experimentally studied the relationship between shear stress and shear rate for non-Newtonian fluids [10], [11], [12]. The authors of [13] have presented the flow rate in pipe formula for Herschel-Bulkley fluids, however, the full derivation has not been provided, and the impact of non-Newtonian parameters has not been analyzed in detail. In the work [14], an analytical formula has been derived that determines the velocity distribution for Bingham fluids in annulus for flow in curved (angular) direction. The purpose of this work is to:

- Present a full mathematical derivation of the velocity distribution for Herschel-Bulkley fluids flowing in a pipe
- Present a full mathematical derivation of the velocity distribution for Bingham fluids flowing in annulus
- Based on the velocity distributions derive a formula that calculates the fluid flow rate
- Analyze the influence of various non-Newtonian parameters on the velocity distribution

II. Velocity distribution derivation and analysis

The balance of forces acting on a cylindrical element in z-direction (along the pipe) can be expressed as follows [15]:

$$\frac{\sigma_{rz}}{r}+\frac{\partial\sigma_{rz}}{\partial r}+\frac{1}{r}\frac{\partial\sigma_{\theta z}}{\partial\theta}+\frac{\partial\sigma_{zz}}{\partial z}+\rho Z=\rho\frac{dv_z}{dt}. \quad (1)$$

Here θ, r, z – are cylindrical coordinates, t is time, σ_{rz} is the shear stress that is perpendicular to the r-direction and directed in the z-direction, $\sigma_{\theta z}$ is the shear stress that is perpendicular to the θ-direction and directed in the z-direction, σ_{zz} is the normal stress in z-direction, ρ is fluid density, Z is the acceleration in the z-direction, and v_z is the velocity in z-direction. The well-known Navier-Stokes equations [16] for Newtonian fluids are derived from the balance of forces formula given above.

In this work, we consider steady-state laminar flow of incompressible non-Newtonian fluids in a pipe. We assume that flow exists only in the z-direction, and the velocity is not dependent on θ. Due to the steady state, $\frac{dv_z}{dt}$ becomes 0, and $\frac{\partial\sigma_{\theta z}}{\partial\theta}$ becomes 0 due the symmetrical flow. $\frac{\partial v_z}{\partial z}$ is also equal to 0 since the fluid is assumed to be incompressible. We also express the normal stress in z-direction as σ_{zz} = -P, where P is fluid pressure. According to the Herschel-Bulkley model, the shear

stress σ_{rz} can be expressed as [17]:

$$\sigma_{rz} = -\tau_0 + K\left(\frac{\partial v_r}{\partial z} + \frac{\partial v_z}{\partial r}\right)^n. \quad (2)$$

As there is no flow in r-direction, the term $\frac{\partial v_r}{\partial z}$ is neglected and as a result we get:

$$\sigma_{rz} = -\tau_0 + K\left(\frac{\partial v_z}{\partial r}\right)^n. \quad (3)$$

Firstly, we need to determine the relationship between the shear stress σ_{rz} and the pressure gradient. Considering everything written above, equation (1) is transformed into the following ordinary differential equation:

$$\frac{\sigma_{rz}}{r} + \frac{d\sigma_{rz}}{dr} - \frac{dP}{dz} + \rho Z = 0. \quad (4)$$

The following assumptions are made in equation (4):

- σ_{rz} is considered to be only a function of r and it is not dependent on coordinates z and θ.
- The pressure gradient $\frac{dP}{dz}$ only dependents on the coordinate z and it is not dependent on r and θ.

Then the solution of the equation (4) would look as follows:

$$\sigma_{rz} = \frac{c_1}{r} + \frac{r}{2}\left(\frac{dP}{dz} - \rho Z\right). \quad (5)$$

Further solution of this equation depends on the chosen boundary conditions. Firstly, we will consider flow in a pipe of radius R. In case of a pipe, r = 0 is a valid coordinate, however, it leads to an infinite σ_{rz} in equation (5) which is not possible. For this reason, c_1 must be taken as 0, and as a result we get:

$$\sigma_{rz} = \frac{r}{2}\left(\frac{dP}{dz} - \rho Z\right). \quad (6)$$

From this equation, we can conclude that the shear stress is equal to 0 in the center of the pipe, and it has the maximum value at the pipe radius R.

The next goal is to determine the relationship between fluid velocity and r. For this, we insert equation (3) into equation (4), and as a result we get the following:

$$-\frac{\tau_0}{r} + \frac{K}{r}\left(\frac{dv}{dr}\right)^n + Kn\left(\frac{dv}{dr}\right)^{n-1}\frac{d^2v}{dr^2} = \frac{dP}{dz} - \rho Z. \quad (7)$$

Now let's assume that $\frac{dv}{dr} = w$, $\frac{d^2v}{dr^2} = \frac{dw}{dr}$, add the term $\frac{\tau_0}{r}$ to left and right side and divide both sides by K:

$$n\frac{dw}{dr}w^{n-1} + \frac{w^n}{r} = \frac{\tau_0 + r\left(\frac{dP}{dz} - \rho Z\right)}{Kr}. \quad (8)$$

Let's assume that $w^n = u$, $nw^{n-1}\frac{dw}{dr} = \frac{du}{dr}$. Then we get:

$$\frac{du}{dr} + \frac{u}{r} = \frac{\tau_0 + r\left(\frac{dP}{dz} - \rho Z\right)}{Kr}. \quad (9)$$

Equation (9) can be transformed as follows:

$$d(ru) = \frac{\tau_0 + r\left(\frac{dP}{dz} - \rho Z\right)}{K}dr. \quad (10)$$

By integrating both sides of this equation we get:

$$ru = \frac{\tau_0 r + \frac{r^2}{2}\left(\frac{dP}{dz} - \rho Z\right)}{K} + c_1. \quad (11)$$

By solving for u, we get:

$$u = \frac{\tau_0 + \frac{r}{2}\left(\frac{dP}{dz} - \rho Z\right)}{K} + \frac{c_1}{r}. \quad (12)$$

Then u is transformed back into w:

$$w = \sqrt[n]{\frac{\tau_0 + \frac{r}{2}\left(\frac{dP}{dz} - \rho Z\right)}{K} + \frac{c_1}{r}}. \quad (13)$$

Then w is transformed back to v:

$$\frac{dv}{dr} = \sqrt[n]{\frac{\tau_0 + \frac{r}{2}\left(\frac{dP}{dz} - \rho Z\right)}{K}} + \frac{c_1}{r}. \tag{14}$$

Since r = 0 leads to an infinite $\frac{dv}{dr}$, the constant c_1 needs to be made equal to 0:

$$\frac{dv}{dr} = \sqrt[n]{\frac{\tau_0 + \frac{r}{2}\left(\frac{dP}{dz} - \rho Z\right)}{K}}. \tag{15}$$

Considering that $\frac{dP}{dz}$ always has a negative value, and that the term $\tau_0 + \frac{r}{2}\frac{dP}{dz}$ has to always be positive, in order for $\frac{dv}{dr}$ to remain a real number, we rewrite the equation (15) as follows:

$$\frac{dv}{dr} = -\sqrt[n]{\frac{-\frac{r}{2}\left(\frac{dP}{dz} - \rho Z\right) - \tau_0}{K}}. \tag{16}$$

From equation (6), we can conclude that in order for a fluid layer located at coordinate r to move relative to neighboring layers, the following condition has to be satisfied:

$$\left|\frac{r}{2}\left(\frac{dP}{dz} - \rho Z\right)\right| > \tau_0. \tag{17}$$

The solution of differential equation (16) is as follows:

$$v = c_2 - \frac{n}{n+1}\sqrt[n]{\frac{-\frac{r}{2}\left(\frac{dP}{dz} - \rho Z\right) - \tau_0}{K}}\left(\frac{2\tau_0}{\frac{dP}{dz} - \rho Z} + r\right). \tag{18}$$

As indicated previously, the shear stress has a minimum value in the center of the pipe, and it increases with the increase of radius. Since we are considering a fluid that has a yield stress τ_0, there has to be a certain radius r_c in the pipe until which the shear stress that occurs in the fluid does not exceed the yield stress. Therefore, a certain flow region from r=0 to r=r_c is formed where the shear stress is less than τ_0. This region can be called the core of the flow, and it is moving through the pipe as a whole, meaning that the layers within this core do not move relative to each other. The core of the flow has a certain velocity v_c which is the maximum velocity in the pipe. In the flow region from r=r_c to r=R the velocity gradually decreases and becomes equal to 0 at r=R and we can refer to this region as out-of-core region. All of this can be summarized in the following equations:

$$r_c = \left|\frac{2\tau_0}{\frac{dP}{dz} - \rho Z}\right|, \tag{19}$$

$$\left|\frac{2\tau_0}{\frac{dP}{dz} - \rho Z}\right| < R. \tag{20}$$

Equation (19) shows the formula for determination of the radius of the core. We can see that the core radius increases with the increase of yield stress and decreases with the increase of the pressure gradient. Equation (20) shows the condition of flow in a pipe in general. In other words, in order for flow to occur in the pipe, the radius of the core needs to be smaller than the radius of the pipe.

Next, we shall determine the constant c_2 in equation (18) by using the conditions described above. Due to the fact that the velocity is equal to 0 at r = R, we get:

$$0 = c_2 - \frac{n}{n+1}\sqrt[n]{\frac{-\frac{R}{2}\left(\frac{dP}{dz} - \rho Z\right) - \tau_0}{K}}\left(\frac{2\tau_0}{\frac{dP}{dz} - \rho Z} + R\right). \tag{21}$$

From here we get that the constant c_2 is determined as:

$$c_2 = \frac{n}{n+1}\sqrt[n]{\frac{-\frac{R}{2}\left(\frac{dP}{dz} - \rho Z\right) - \tau_0}{K}}\left(\frac{2\tau_0}{\frac{dP}{dz} - \rho Z} + R\right). \tag{22}$$

Finally, we derive the equation that describes the velocity distribution in a pipe for Herschel-Bulkley fluids:

$$v = \frac{n}{n+1}\sqrt[n]{\frac{-\frac{R}{2}\left(\frac{dP}{dz}-\rho Z\right)-\tau_0}{K}}\left(\frac{2\tau_0}{\frac{dP}{dz}-\rho Z}+R\right)-\frac{n}{n+1}\sqrt[n]{\frac{-\frac{r}{2}\left(\frac{dP}{dz}-\rho Z\right)-\tau_0}{K}}\left(\frac{2\tau_0}{\frac{dP}{dz}-\rho Z}+r\right). \quad (23)$$

If we insert r=r_c into the equation above and use the definition of r_c from equation (19), we will get the following formula for finding the velocity of the core of the flow:

$$v_c = \frac{n}{n+1}\sqrt[n]{\frac{-\frac{R}{2}\left(\frac{dP}{dz}-\rho Z\right)-\tau_0}{K}}\left(\frac{2\tau_0}{\frac{dP}{dz}-\rho Z}+R\right). \quad (24)$$

By knowing the velocity distribution, we can determine the flow rate in the pipe using the formula below:

$$Q = Q_c + Q_{oc}, \quad (25)$$

where Q_c is the flow rate of the core region and Q_{oc} is the flow rate of out-of-core region. Q_c is determined as:

$$Q_c = \pi r_c^2 v_c = \pi\left(-\frac{2\tau_0}{\frac{dP}{dz}-\rho Z}\right)^2 \frac{n}{n+1}\sqrt[n]{\frac{-\frac{R}{2}\left(\frac{dP}{dz}-\rho Z\right)-\tau_0}{K}}\left(\frac{2\tau_0}{\frac{dP}{dz}-\rho Z}+R\right). \quad (26)$$

On the other hand, Q_{oc} is determined as:

$$Q_{oc} = \int_{r_c}^{R} v d(\pi r^2) = \int_{r_c}^{R} 2\pi v r dr. \quad (27)$$

By calculating this integral and summing up Q_c and Q_{oc}, we get the following final formula for flow rate in pipe:

$$Q = \frac{\pi n}{K^{\frac{1}{n}}}\frac{\left(-\frac{R}{2}\left(\frac{dP}{dz}-\rho Z\right)-\tau_0\right)^{1+\frac{1}{n}}}{\left(-\frac{1}{2}\left(\frac{dP}{dz}-\rho Z\right)\right)^3}\left(\frac{\left(-\frac{R}{2}\left(\frac{dP}{dz}-\rho Z\right)-\tau_0\right)^2}{3n+1}+\frac{2\tau_0\left(-\frac{R}{2}\left(\frac{dP}{dz}-\rho Z\right)-\tau_0\right)}{2n+1}+\frac{\tau_0^2}{n+1}\right). \quad (28)$$

Figure 1 (a) shows the velocity distribution in pipe in 3D built based on equation (23) for Herschel-Bulkley fluids (τ_0=20 Pa, n=1.2). Due the presence of yield stress, a core region of radius r_c is formed in the center of the pipe which has maximum velocity.

Figure 1 (b) shows various distributions of fluid velocity in pipe for different values of pressure gradient. It can be seen that the increase of pressure gradient leads to the increase of velocity in every coordinate, and it decreases the radius r_c of the core.

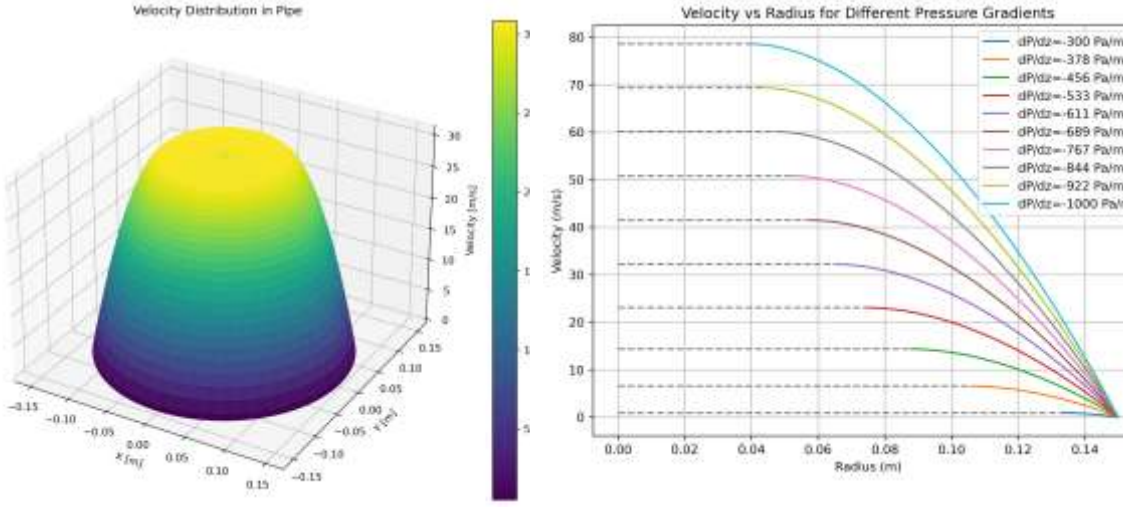

(a) (b)

Figure 1: *Velocity distribution in pipe in 3D (a); Velocity distributions in pipe for different pressure gradients (b)*

Figure 2 (a) shows various distributions of fluid velocity in pipe for different values of consistency index. It can be seen that the decrease of the consistency index increases velocity at every point, however, it does not affect the core radius. Moreover, the increase of velocity with the decrease of the consistency index is higher for lower consistency indexes.

Figure 2 (b) shows various distributions of fluid velocity in pipe for different values of yield stress. The decrease of yield stress increases velocity at every point and decreases the radius of the core region. The increase of velocity with the decrease of yield stress is higher for lower yield stresses.

Figure 2 (c) shows the relationship between core velocity, pressure gradient and power-law index n. The key observation here is that the relationship between core velocity and power-law index depends on the pressure gradient. At low pressure gradients the velocity increases with the increase of n, while at high pressure gradients the velocity increases with the decrease of n.

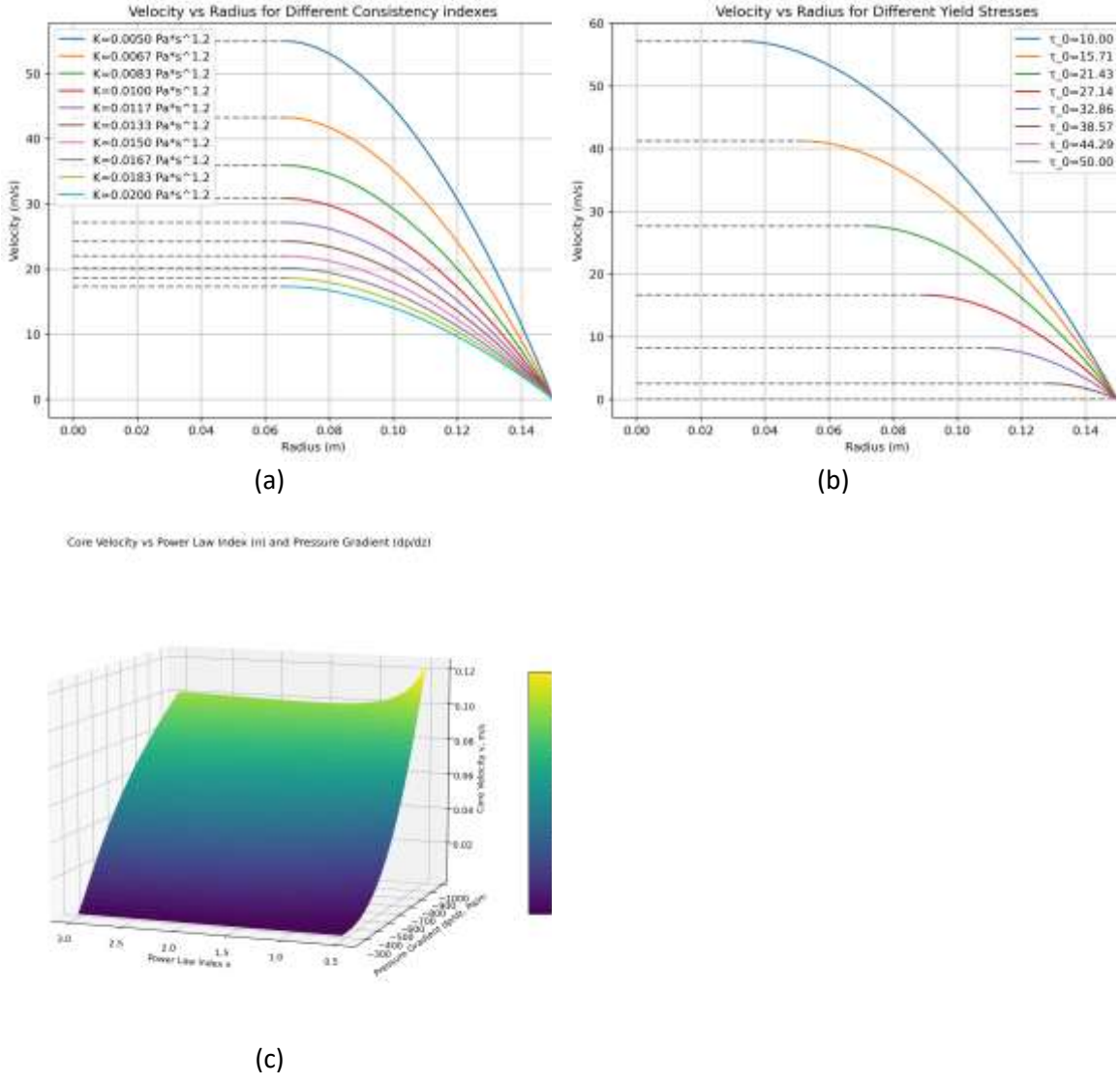

Figure 2: *Velocity distributions in pipe for different consistency indexes (a); Velocity distributions in pipe for different yield stresses (b); Relationship between velocity, pressure gradient and power-law index in 3D (c)*

Next, we shall analyze the flow of non-Newtonian fluids in annulus. No analytical solution for Herschel-Bulkley fluids in annulus was found, however, we derived an analytical solution for Bingham fluids in annulus.

In annulus, the flow occurs between the inner radius R_1 and the outer radius R_2. The core region of the flow should be located between the radiuses r_{c1} and r_{c2}. Those radiuses correspond to the conditions $R_1 < r_{c1} < r_{c2} < R_2$. As in previous case, here we start with the analysis of the shear stress formula:

$$\sigma_{rz} = \frac{c_1}{r} + \frac{r}{2}\left(\frac{dP}{dz} - \rho Z\right) \tag{29}$$

When r=r_{c1} the shear stress becomes equal to -τ_0, so we get the following:

$$-\tau_0 = \frac{c_1}{r_{c1}} + \frac{r_{c1}}{2}\left(\frac{dP}{dz} - \rho Z\right) \tag{30}$$

From here we find that the constant c_1 is equal to:

$$c_1 = -\tau_0 r_{c1} - \frac{{r_{c1}}^2}{2}\left(\frac{dP}{dz} - \rho Z\right) \tag{31}$$

So, we get the following equation for the shear stress:

$$\sigma_{rz} = \frac{-\tau_0 r_{c1} - \frac{{r_{c1}}^2}{2}\left(\frac{dP}{dz} - \rho Z\right)}{r} + \frac{r}{2}\left(\frac{dP}{dz} - \rho Z\right) \tag{32}$$

Next, we can insert r=r_{c2} to the shear stress equation and it should also lead to σ_{rz}=$-\tau_0$:

$$-\tau_0 = \frac{-\tau_0 r_{c1} - \frac{{r_{c1}}^2}{2}\left(\frac{dP}{dz} - \rho Z\right)}{r_{c2}} + \frac{r_{c2}}{2}\left(\frac{dP}{dz} - \rho Z\right) \tag{33}$$

From here we get the following relationship between r_{c2} and r_{c1}:

$$r_{c2} = \frac{-\tau_0 - \sqrt{{\tau_0}^2 + 2\left(\tau_0 r_{c1} + \frac{{r_{c1}}^2}{2}\left(\frac{dP}{dz} - \rho Z\right)\right)\left(\frac{dP}{dz} - \rho Z\right)}}{\frac{dP}{dz} - \rho Z} \tag{34}$$

Next, we use the formula for velocity gradient derived earlier to proceed further (we set n=1):

$$\frac{dv}{dr} = \frac{\tau_0 + \frac{r}{2}\left(\frac{dP}{dz} - \rho Z\right)}{K} + \frac{c_1}{r} \tag{35}$$

We should have 2 independent solutions for the flow region between R_1&r_{c1} and between R_2&r_{c2}. Let's first consider the first region. In this case, the velocity gradient at r_{c1} will be equal to 0, so we get:

$$0 = \frac{\tau_0 + \frac{r_{c1}}{2}\left(\frac{dP}{dz} - \rho Z\right)}{K} + \frac{c_1}{r_{c1}} \tag{36}$$

From here we get that c_1 is equal to:

$$c_1 = -\frac{\tau_0 r_{c1} + \frac{{r_{c1}}^2}{2}\left(\frac{dP}{dz} - \rho Z\right)}{K} \tag{37}$$

The integration of the velocity gradient equation gives the following result:

$$v = \frac{\frac{r^2}{2}\left(\frac{dP}{dz} - \rho Z\right) + 2c_1 K ln(r) + 2r\tau_0}{2K} + c_2 \tag{38}$$

Since at r=R_1 the velocity becomes equal to 0, then we get:

$$0 = \frac{\frac{{R_1}^2}{2}\left(\frac{dP}{dz} - \rho Z\right) + 2c_1 K ln(R_1) + 2R_1\tau_0}{2K} + c_2 \tag{39}$$

So, the constant c_2 is equal to:

$$c_2 = -\frac{\frac{{R_1}^2}{2}\left(\frac{dP}{dz} - \rho Z\right) + 2c_1 K ln(R_1) + 2R_1\tau_0}{2K} \tag{40}$$

So, the final velocity distribution equation after simplification would look as follows (minus is added to account for the fact that the velocity gradient is positive in the region from R_1 to r_{c1}):

$$v = -\frac{\frac{\left(r^2 - {R_1}^2\right)}{2}\left(\frac{dP}{dz} - \rho Z\right) - 2\left(\frac{\tau_0 r_{c1} + \frac{{r_{c1}}^2}{2}\left(\frac{dP}{dz} - \rho Z\right)}{K}\right) K ln\left(\frac{r}{R_1}\right) + 2\tau_0(r - R_1)}{2K} \tag{41}$$

Similarly, for the second out-of-core region we would get:

$$v = \frac{\frac{\left(r^2 - {R_2}^2\right)}{2}\left(\frac{dP}{dz} - \rho Z\right) - 2\left(\frac{\tau_0 r_{c2} + \frac{{r_{c2}}^2}{2}\left(\frac{dP}{dz} - \rho Z\right)}{K}\right) K ln\left(\frac{r}{R_2}\right) + 2\tau_0(r - R_2)}{2K} \quad (42)$$

At this point we have 1 unknown, which is the r_{c1} (because the relationship between r_{c1} and r_{c2} is already known). To find r_{c1} we use the boundary condition that the velocity in the first region at r=r_{c1} should be equal to the velocity in the second region at r=r_{c2}. Then we express r_{c2} in terms of r_{c1} and solve the equation for r_{c1}. However, mathematically this is very complex, and we suggest using numerical approaches to find the value of r_{c1}.

For annular flow, the condition for a certain layer to move relative to neighboring layers is:

$$\left|\frac{-\tau_0 r_{c1} - \frac{{r_{c1}}^2}{2}\left(\frac{dP}{dz} - \rho Z\right)}{r} + \frac{r}{2}\left(\frac{dP}{dz} - \rho Z\right)\right| > \tau_0 \quad (43)$$

The general flow condition in annulus is:

$$R_1 < r_{c1} < r_{c2} < R_2 \quad (44)$$

Obviously, the values of r_{c1} and r_{c2} depend on the value of the pressure gradient. When the pressure gradient increases then the values of r_{c1} and r_{c2} become closer.

The flow rate in annulus is determined using the formula:

$$Q = Q_c + Q_{oc1} + Q_{oc2} \quad (45)$$

where Q_c is the flow rate of the core region, and Q_{oc1}&Q_{oc2} are flow rates of out-of-core regions. Q_c is determined using the formula:

$$Q_c = \pi(r_{c2}^2 - r_{c1}^2)v_c \quad (46)$$

Here v_c can be found by inserting either r_{c1} in the first velocity distribution equation or r_{c2} in the second velocity distribution equation.

On the other hand, Q_{oc1} is determined using the formula below:

$$Q_{oc1} = 2\pi \int_{R_1}^{r_{c1}} vrdr \quad (47)$$

Integration results in the following:

$$Q_{oc1} = -\frac{\pi r^2\left(6\left(\tau_0 r_{c1} + \frac{{r_{c1}}^2}{2}\left(\frac{dP}{dz} - \rho Z\right)\right)\left(1 - 2ln\left(\frac{r}{R_1}\right)\right) - 3{R_1}^2\left(\frac{dP}{dz} - \rho Z\right) - 12R_1\tau_0 + \frac{3}{2}\left(\frac{dP}{dz} - \rho Z\right)r^2 + 8r\tau_0\right)}{12K}\Big|_{R_1}^{r_{c1}} \quad (48)$$

Similarly, for Q_{oc2} we have:

$$Q_{oc2} = 2\pi \int_{r_{c2}}^{R_2} vrdr \quad (49)$$

And integration gives the following result:

$$Q_{oc2} = \frac{\pi r^2\left(6\left(\tau_0 r_{c2} + \frac{{r_{c2}}^2}{2}\left(\frac{dP}{dz} - \rho Z\right)\right)\left(1 - 2ln\left(\frac{r}{R_2}\right)\right) - 3{R_2}^2\left(\frac{dP}{dz} - \rho Z\right) - 12R_2\tau_0 + \frac{3}{2}\left(\frac{dP}{dz} - \rho Z\right)r^2 + 8r\tau_0\right)}{12K}\Big|_{r_{c2}}^{R_2} \quad (50)$$

Figure 3 (a) shows the velocity distribution in annulus in 3D for Bingham fluids (τ_0=300 Pa, n=1). It can be seen that the velocity is equal to 0 at the inner and outer boundaries of the annulus and it quite abruptly increases to the maximum value which corresponds to the core of the flow.

Figure 3 (b) shows various distributions of fluid velocity in annulus for different values of pressure gradient. Despite the fact that the pressure gradient varies in a small interval, it significantly affects the velocity profile. At pressure gradient equal to -520 Pa/m flow is absent while at -625 Pa/m the velocity is very high, and the radius of the core is very small. Another observation is that the velocity increases more abruptly in the inner part of the annulus (between the annulus inner radius and the core inner radius) than in the outer part of the annulus (between the core outer radius and the annulus outer radius).

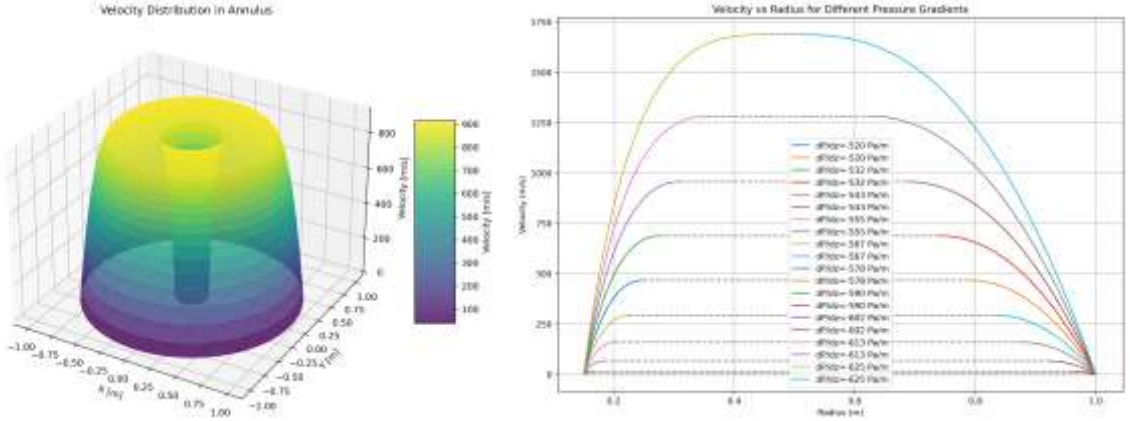

Figure 3: *Velocity distribution in annulus in 3D (a); Velocity distributions in annulus for different pressure gradients (b)*

Fig.4 (a) shows various distributions of fluid velocity in annulus for different values of consistency index. It can be seen that decrease of the consistency index significantly increases velocity but does not affect the inner and outer radiuses of the core.

Fig.4 (b) shows various distributions of fluid velocity in annulus for different values of yield stress. The yield stress changes in a very small interval (from 250 to 300 Pa), however, the sensitivity of the velocity profile to yield stress is very high, as it increases from 0 at τ_0=300 Pa to a very high value at τ_0=250 Pa, at which the size of the core becomes very small.

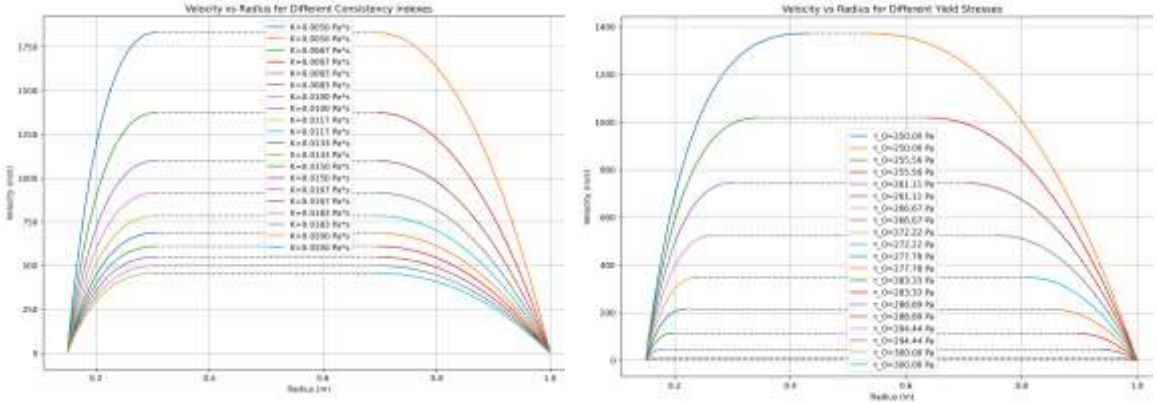

Fig.4: *Velocity distributions in annulus for different consistency indexes (a); Velocity distributions in annulus for different yield stresses (b)*

III. Conclusion

The purpose of this work was to study the flow of non-Newtonian fluids in pipe and annulus and analyze the impact of non-Newtonian parameters on the flow. Firstly, the velocity distribution in pipes for Herschel-Bulkley fluids has been derived based on the balance of forces equation. It has been shown that the flow of yield stress fluids is characterized by presence of a certain region (core of the flow) that moves as a whole (layers do not move relative to each other) which has the maximum velocity. Moreover, the flow condition for such fluids in a pipe has been presented and the formula to determine the overall flow rate in the pipe has been derived.

Next, the impact of non-Newtonian parameters on the velocity distribution in a pipe was graphically analyzed. The conclusion was that the decrease of the consistency index significantly increases the velocity, however, it does not affect the size of the core. On the other hand, the decrease

of the yield stress strongly increases velocity and decreases the size of the core. The most interesting finding of this work is that the relationship between the velocity and the power-law index depends on the pressure gradient. At low pressure gradients the increase of power-law index increases velocity, while at high pressure gradients it is the opposite.

No analytical solution for velocity distribution was found for Herschel-Bulkley fluids in annulus, however, a solution has been derived for Bingham fluids. It has been shown that similar to the case with the pipe, in annulus a core region is present as well and it is characterized by 2 radiuses – inner and outer radius of the core that are located between the inner and outer radius of the annulus. It has been concluded that the velocity is very sensitive to even small changes in yield stress and pressure gradient. Another conclusion is that the velocity increases more abruptly between the inner radius of the annulus and the core compared with the velocity in the region between the core and the outer radius of the annulus.

CONFLICT OF INTEREST.

Authors declare that they do not have any conflict of interest.

References

[1] Yatimi Y., Mendil J., Marafi M., Alalou A., Al-Dahhan M.H.. Advancement in heavy oil upgrading and sustainable exploration emerging technologies, 2024 // Arabian Journal of Chemistry, 17(3), https://doi.org/10.1016/j.arabjc.2024.105610 .

[2] Muther T. et al. Unconventional hydrocarbon resources: geological statistics, petrophysical characterization, and field development strategies, 2021 // Journal of Petroleum Exploration and Production Technology, 12, p. 1463-1488, https://doi.org/10.1007/s13202-021-01404-x .

[3] Zyrin V.l., Ilinova A. Ecology safety technologies of unconventional oil reserves recovery for sustainable oil and gas industry development, 2016 - // J. Ecol. Eng., 17(4), p. 35-40, https://doi.org/10.12911/22998993/64637 .

[4] Rehm B., Haghshenas A., Paknejad A., Al-Yami A., Hughes J., Schubert J.. Underbalanced Drilling: Limits and Extremes, 2012 - Gulf Publishing Company, ISBN: 9780127999807.

[5] Panton R.L. Incompressible Flow, 2013 - Hoboken: John Wiley & Sons, ISBN: 978-1-118-41573-3.

[6] Coussot P.. Bingham's heritage, 2017 - Rheologica Acta, 56, p. 163-176, https://doi.org/10.1007/s00397-016-0983-y .

[7] Pierre S. Cham. Complex fluids: Modeling and Algorithms, 2016 - Switzerland: Springer International Publishing, https://doi.org/10.1007/978-3-319-44362-1, ISBN: 978-3-319-44362-1.

[8] Tang Hansong S., Kalyon Dilhan M. Estimation of the parameters of Herschel–Bulkley fluid under wall slip using a combination of capillary and squeeze flow viscometers, 2004 - Rheologica Acta, 43(1), p. 80–88, https://doi.org/10.1007/s00397-003-0322-y .

[9] Kfuri S., Soares E., Thompson R., Siqueira R.. Friction Coefficients for Bingham and Power-Law Fluids in Abrupt Contractions and Expansions, 2016 - Journal of Fluids Engineering, 139(2), https://doi.org/10.1115/1.4034521 .

[10] Chevalier T., et al. Darcy's law for yield stress fluid flowing through a porous medium, 2013 - Journal of Non-Newtonian Fluid Mechanics, 195, p. 57-66, https://doi.org/10.1016/j.jnnfm.2012.12.005 .

[11] Danov K.D. On the viscosity of dilute emulsions, 2001 - Journal of Colloid And Interphase Science. , 235, p. 144-149, https://doi.org/10.1006/jcis.2000.7315 .

[12] Kelbaliyev G. I., Tagiyev D. B., Manafov M. R.. Rheology of Heavy Oils, 2022 - Web of Science, http://dx.doi.org/10.5772/intechopen.105666 .

[13] Mitchell, R. F., Miska S. Z. Fundamentals of drilling engineering, 2011 - SPE textbook series no. 12, ISBN: 1555632076.

[14] Roberts T.G., Cox S.J. An analytic velocity profile for pressure-driven flow of a Bingham

fluid in a curved channel, 2020 - Journal of Non-Newtonian Fluid Mechanics, 280, https://doi.org/10.1016/j.jnnfm.2020.104278 .

[15] Vitturi M. D. Navier-Stokes equations in cylindrical coordinates derivation of the equations, 2022 - INGV Pisa, Italy.

[16] McLean D. Continuum Fluid Mechanics and the Navier-Stokes Equations, 2012 - John Wiley & Sons, p. 13–78, http://dx.doi.org/10.1002/9781118454190.ch3 .

[17] Chambon G., Ghemmour A., Naaim M. Experimental investigation of viscoplastic free-surface flows in a steady uniform regime, 2014 - Journal of Fluid Mechanics Mechanics, 754, p. 332—364, http://dx.doi.org/10.1017/jfm.2014.378 .